

# Programmable integrated photonic circuit for matrix inversion

G. Cavicchioli<sup>1,\*</sup>, D. A. B. Miller<sup>2</sup>, N. Engheta<sup>3</sup>, A. Melloni<sup>1</sup>, and F. Morichetti<sup>1</sup>

<sup>1</sup> Dipartimento di elettronica informazione e bioingegneria, Politecnico di Milano, Via Ponzio 34/5, 20133 Milano, Italy

<sup>2</sup> Ginzton Laboratory, Spilker Building, Stanford University, Stanford, CA 94305, USA

<sup>3</sup> Department of Electrical and Systems Engineering, University of Pennsylvania, Philadelphia, Pennsylvania, 19104, USA

\*gabriele.cavicchioli@polimi.it

**Abstract:** We propose and demonstrate the optical inversion of a programmable matrix by using a silicon photonic interferometer mesh in a feedback loop, without any optical-to-electronic conversions inside the inversion process. © 2023 The Author(s)

## 1. Introduction

Photonic computing is becoming a valuable alternative to digital electronic circuits in those fields that require high speed and low power consumption in solving mathematical problems [1]. In particular, Programmable Optical Processors (POPs) provide an efficient analogue version of matrix-vector-multiplication (MVM) [2] that has already been exploited for machine learning applications [3]. POPs are inherently analogue devices [4]: the inputs and the outputs are arrays of optical signals that must be converted in and out of the digital domain. This digitization must be done using electronics circuits, which can then become the bottleneck in such processors. Hence, many mathematical problems cannot benefit fully from such POPs. It is therefore critical to extend the range of mathematical operations that can be implemented in optics without requiring such electro-optical conversions.

In this work we present the design of a recursive programmable photonic solver that can perform inversion of programmable matrices [5]. In particular, we explain the proposed architecture and how it can invert a given matrix, we show supporting numerical simulations, and we finally show a silicon photonic realization of the proposed circuit providing an experimental demonstration of all-optical matrix inversion.

## 2. Recursive MZI mesh for matrix inversion

Figure 1(a) shows the schematic of the programmable photonic solver employed in this work. It consists of  $N = 3$  optical loops which are coupled by a reconfigurable  $N \times N$  mesh of Mach-Zehnder interferometers (MZIs), as shown in Fig. 1(b). The MZI mesh forms the reconfigurable *kernel*  $K$  of the system, and can implement any  $N \times N$  unitary linear operator [6]. A key aspect of the matrix inversion is that we feed the output of the mesh controllably back to the input. These loops also have input waveguide ports ( $X_i$ ) for feeding a vector into the architecture and output waveguide ports ( $Y_i$ ) for reading the output vector. These ports use optical couplers; the input couplers are labelled as *Through* couplers, while the output couplers are labelled as *Drop* couplers. Because of the feedback loop, the frequency domain transfer function  $T_d$  at the drop port is given by

$$T_d = D_{12} e^{-j\phi_d} \frac{1}{I - e^{-j\omega' T_{22} K D_{22}}} T_{21}, \quad (1)$$

where  $T_{ij}$  and  $D_{ij}$  are the transfer matrices of the Through and Drop couplers, respectively (see Fig. 1(c)),  $\phi_d$  is the phase delay between the Through and the Drop couplers, and  $\omega' = \omega / \text{FSR}$  is the frequency normalized to the free spectral range (FSR) of the circuit, which takes into account the round trip phase of the loop. Equation (1) shows that, when  $\omega' = 2M\pi$ , the transfer matrix  $T_d$  is proportional to the inverse matrix of  $I - K_{\text{eff}}$ , where  $K_{\text{eff}} = T_{22} K D_{22}$  is the effective kernel of the circuit, that is scaled by the extrinsic loss due to the input  $T_{22}$  and output  $D_{22}$  coupling with the external waveguides [7]. If we were to excite the circuit sequentially with input vectors  $X_1 = (1, 0, 0)$ ,  $X_2 = (0, 1, 0)$ , and  $X_3 = (0, 0, 1)$ , the output vectors  $Y_1$ ,  $Y_2$ , and  $Y_3$  would correspond respectively to the columns of the transfer matrix  $T_d$  and so they are proportional to the inverse of  $I - K_{\text{eff}}$ . Therefore, to solve for the inverse of a given matrix  $A$ , we need to set the kernel of the circuit such that

$$K_{\text{eff}} = I - A, \quad (2)$$

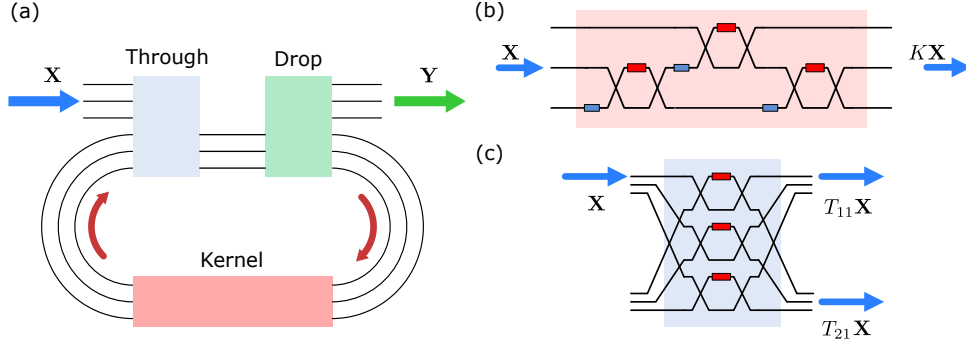


Fig. 1: (a) Schematic of the proposed programmable optical processor. (b) Kernel of the processor realized with a programmable MZI mesh. Each MZI in the mesh has two phase shifters (red and blue boxes in the inset) and can be reconfigured to change the operator implemented by the kernel. (c) Array of MZI tunable couplers used to couple light into and out of the solver.

and this is always possible since  $K$  can be any linear operator. Actually, in practice  $K$  is limited to matrices without internal gain, so the realization of a kernel is limited by the loss of the cavities, including the losses of the couplers. Such limitation could be removed if the circuit was fabricated in a photonic platform including optical amplifiers.

Figure 2 shows a simulation based on the transfer matrix method (TMM) of the frequency response of the circuit. The numerical analysis is carried out considering a photonic circuit with optical feedback (technically therefore forming three optical resonators) coupled with a triangular mesh as shown in Fig. 1(b). In the simulation the kernel is set to

$$K = \begin{pmatrix} 1 & 0 & 0 \\ 0 & 1/\sqrt{2} & -1/\sqrt{2} \\ 0 & -1/\sqrt{2} & -1/\sqrt{2} \end{pmatrix}, \quad (3)$$

while the round trip loss of the resonators is assumed equal to 20 % (that is, about 1 dB per round trip). The coupling ratios of the Through and Drop port couplers are assumed to be 37.5 % and 10 % respectively. According to (1), the modulus square of the inverse matrix computed by the circuit is given by the Hadamard product

$$H_d = T_d \circ T_d^* = \begin{pmatrix} 0.124 & 0 & 0 \\ 0 & 0.102 & 0.006 \\ 0 & 0.006 & 0.027 \end{pmatrix}, \quad (4)$$

which corresponds to the intensity transfer function evaluated for  $\omega = 0$  as shown by the markers in Fig. 2.

A prototype of the photonic solver was fabricated in a commercial 220-nm Silicon Photonics (SiPh) platform. A photo of the device is shown in Fig. 3(a). In this circuit, variable Through couplers are realized by means of tuneable MZIs, while fixed Drop couplers are made from tap directional couplers with a 10 % power coupling ratio. The three feedback loops share the same length of 5.7 mm (including the kernel MZI mesh), resulting in a

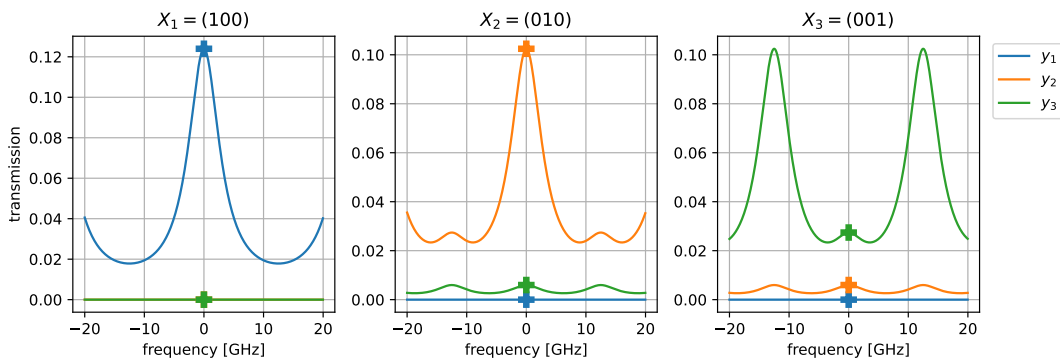


Fig. 2: Simulation of the transfer matrix of the solver between the input and the drop port. The marker corresponds to the modulus squared elements of the inverse matrix.

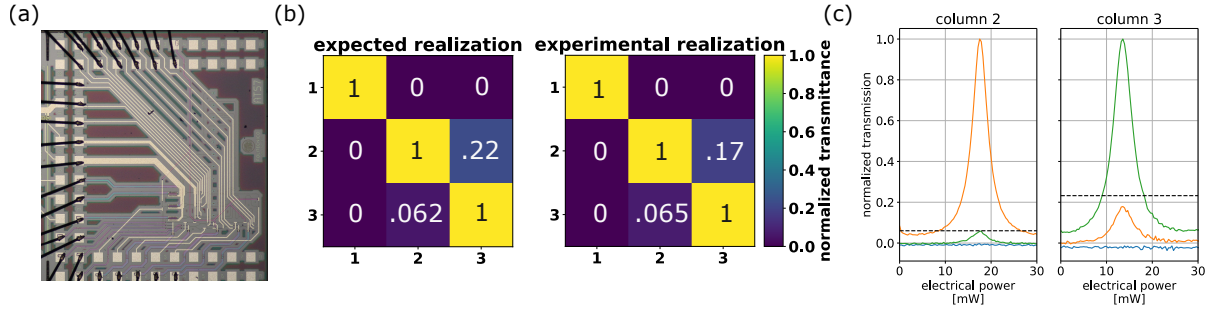


Fig. 3: (a) Microscope Photograph of the SiPh prototype. (b) comparison between expected and experimental inverse matrix (each column is normalized to its maximum to compensate for inhomogeneous coupling loss of the experimental setup). (c) Normalized transmittance at the drop port, varying the resonance frequency through the circuit's phase shifters.

$FSR$  of 12.5 GHz. Thermal phase shifters are used to reconfigure the input MZI couplers and the MZI mesh of the kernel.

Figure 3 reports an experimental validation of matrix inversion, when the state of the kernel and of the input couplers is nominally set to the same values considered in the simulations of Fig. 2. The optical power at the Drop port, namely  $|Y_1|^2$ ,  $|Y_2|^2$ ,  $|Y_3|^2$ , is measured when input vectors  $X_1$ ,  $X_2$ ,  $X_3$  are sequentially used, and provides the column of the matrix  $H_d$ . Figure 3(b) shows the expected matrix  $H_d$  and the corresponding experimental one  $H_{d,exp}$  (each column of the matrices have been normalized to its maximum to compensate for slightly different coupling loss in the input ports of the circuit). A very good agreement is found for all the nine elements of the matrix. Figure 3(c) shows the evolution of the Drop port power (for input vectors  $X_2$  and  $X_3$ ), when the round trip phase of one of the feedback loop is changed by using an integrated phase shifter. The peaks of the curves correspond to the resonance condition ( $\omega' = 2M\pi$ ) and provide the inversion of the matrix whose kernel is the one given eq. (3). The dotted black lines indicate the expected level from simulation and the small deviation from the expected value is due to non-idealities of the fabricated device and some thermal cross-talk between the phase shifters. When the round trip phase of the loop is modified by acting on integrated phase shifters, a phase term is added to the matrix of the kernel, thus leading to the inversion of a different matrix.

### 3. Conclusions

In this work, we have presented the design and operation of a programmable optical processor performing matrix inversion. By exploiting a programmable MZI mesh in a recursive topology, the device can set the matrix to be inverted making it truly programmable. Note that this inversion is performed without optical-to-electronic conversions inside the processor. A prototype has been realized in the SiPh platforms inverting  $3 \times 3$  matrices. Simulation of the prototype and preliminary experimental characterization demonstrate the capabilities of this new architecture.

*This work was supported by the Italian National Recovery and Resilience Plan (NRRP) of NextGenerationEU, "Telecommunications of the Future" (PE00000001 - program "RESTART", Structural Project "Rigoletto" and Focused Project "HePIC") and "MUSA: Multilayered Urban Sustainability Action", and by AFOSR grant FA9550-21-1-0312.*

### References

1. F. Zangeneh-Nejad, D. L. Sounas, A. Alù, and R. Fleury, "Analogue computing with metamaterials," *Nat. Rev. Mater.* **6**, 207–225 (2021).
2. H. Zhou, J. Dong, J. Cheng, W. Dong, C. Huang, Y. Shen, Q. Zhang, M. Gu, C. Qian, H. Chen, Z. Ruan, and X. Zhang, "Photonic matrix multiplication lights up photonic accelerator and beyond," **11**.
3. S. Pai, Z. Sun, T. W. Hughes, T. Park, B. Bartlett, I. A. D. Williamson, M. Minkov, M. Milanizadeh, N. Abebe, F. Morichetti, A. Melloni, S. Fan, O. Solgaard, and D. A. B. Miller, "Experimentally realized in situ backpropagation for deep learning in photonic neural networks," *Science* **380**, 398–404 (2023).
4. A. Macho-Ortiz, D. Pérez-López, J. Azaña, and J. Capmany, "Analog programmable-photonic computation," *Laser & Photonics Rev.* p. 2200360 (2023).
5. D. C. Tzarouchis, M. J. Mencagli, B. Edwards, and N. Engheta, "Mathematical operations and equation solving with reconfigurable metadvice," *Light. Sci. & Appl.* **11**, 263 (2022).
6. D. A. B. Miller, "Self-configuring universal linear optical component," *Photon. Res.* **1**, 1–15 (2013).
7. M. Camacho, B. Edwards, and N. Engheta, "A single inverse-designed photonic structure that performs parallel computing," *Nat. Commun.* **12** (2021). All Open Access, Gold Open Access, Green Open Access.